

Geometric, electronic, and magnetic structure of Co₂FeSi: Curie temperature and magnetic moment measurements and calculations.

Sabine Wurmehl, Gerhard H. Fecher, Hem Chandra Kandpal, Vadim Ksenofontov, and Claudia Felser*
*Institut für Anorganische und Analytische Chemie,
 Johannes Gutenberg - Universität, D-55099 Mainz, Germany.*

Hong-Ji Lin
National Synchrotron Radiation Research Center - NSRRC, Hsinchu, 30076, Taiwan

Jonder Morais
Instituto de Física, Universidade Federal do Rio Grande do Sul, Porto Alegre, 91501-970, Brazil
 (Dated: October 12, 2018)

In this work a simple concept was used for a systematic search for new materials with high spin polarization. It is based on two semi-empirical models. Firstly, the Slater-Pauling rule was used for estimation of the magnetic moment. This model is well supported by electronic structure calculations. The second model was found particularly for Co₂ based Heusler compounds when comparing their magnetic properties. It turned out that these compounds exhibit seemingly a linear dependence of the Curie temperature as function of the magnetic moment.

Stimulated by these models, Co₂FeSi was revisited. The compound was investigated in detail concerning its geometrical and magnetic structure by means of X-ray diffraction, X-ray absorption and Mößbauer spectroscopies as well as high and low temperature magnetometry. The measurements revealed that it is, currently, the material with the highest magnetic moment ($6\mu_B$) and Curie-temperature (1100K) in the classes of Heusler compounds as well as half-metallic ferromagnets. The experimental findings are supported by detailed electronic structure calculations.

PACS numbers: 75.30.-m, 71.20.Be, 61.18.Fs

Keywords: half-metallic ferromagnets, magnetic properties, Heusler compounds, Curie temperature

I. INTRODUCTION

Materials that exhibit half-metallic ferromagnetism are seen to be potential candidates for the field of application being called spintronics^{1,2}, that is electronics making use of the electron spin instead of its charge. The concept of half-metallic ferromagnetism was first presented by de Groot³, predicting it to appear in half Heusler compounds. The model suggests that the density of states exhibits, around the Fermi energy (ϵ_F), a gap for minority electrons. Thus, these materials are supposed to be 100% spin polarized at ϵ_F . Most of the predicted half-metallic ferromagnets (HMF) belong to the Heusler⁴ compounds. In general, these are ternary X_2YZ -compounds crystallizing in the $L2_1$ structure. X and Y are usually transition metals and Z is a main group element.

Beside Heusler compounds, there are only few other materials being predicted to be HMFs, like some oxides. Most of the predicted compounds with Zinblend structure are chemically uncharacterizable, at least up to now. Therefore, our research concentrates on Heusler compounds.

High Curie temperatures, magnetic moments, and large minority gaps are desirable for applications. For room temperature devices, in particular, one needs to prevent a reduction of the spin polarization and other magnetic properties by thermal effects. In this context it should be noted that the Co₂ based Heusler compounds exhibit the highest Curie temperature (985K, Co₂MnSi⁵)

and the highest magnetic moment ($5.54\mu_B$ per unit cell, Co₂FeGe⁵) being reported up to now. The HMF character of Co₂MnZ compounds was first reported by Ishida *et al*⁶. Recently, Co₂MnSi⁷ and Co₂MnGe⁸ were used to built first thin film devices. The present work reports about Co₂FeSi. It will be shown that this compound may be one of the most promising candidates for spintronic applications.

II. THEORETICAL MODELS

There exist several rules counting the number of valence electrons that are used to predict the magnetic moments in Heusler and other magnetic compounds from the number of valence electrons. These rules are based on particular numbers of valence electrons starting with the semi-conducting compounds where one has 18 valence electrons in half Heusler compounds⁹, or 24 in full Heusler compounds. Rules that are not general but depend on the composition of the sample are, somehow, not satisfactory. Therefore, it may be helpful to start more basically. Pauling¹⁰ pointed already on the Heusler alloys in his basic work on the dependence of the magnetic moments in alloys on the number of valence electrons per atom.

Slater¹¹ and Pauling¹⁰ found that the magnetic moments (m) of $3d$ elements and their binary alloys can be described by the mean number of valence electrons per

atom (n_V). The rule distinguishes the dependence of $m(n_V)$ into two regions (see: Fig.1). In the second part ($n_V \geq 8$), one has closed packed structures (fcc, hcp) and m decreases with increasing n_V . This is called the region of itinerant magnetism. According to Hund's rule, it is often favorable that the majority d states are fully occupied ($n_{d\uparrow} = 5$). The magnetic valence is defined by $n_M = 2n_{d\uparrow} - n_V$, such that the magnetic moment per atom is given by $m = n_M + 2n_{sp\uparrow}$. A plot of m versus magnetic valence ($m(n_M)$) is called the generalized Slater-Pauling curve (see Refs.^{12,13}). In the first region ($n_V \leq 8$), m increases with increasing n_V . This part is attributed to localized moments, where Fe (bcc) is a borderline case. Here, the Fermi energy is pinned in a deep valley of the minority electron density. This constrains the number of minority d -electrons $n_{d\downarrow}$ resulting in $m = n_V - 2n_{d\downarrow}$. For Fe and its binary alloys (Fe-Mn, Fe-Cr, and partially Fe-Co) one has an average of approximately three minority electrons occupied with the result $m \approx n_V - 6$. Many Heusler compounds exhibit an increase of m with increasing n_V , and thus they may belong to the first region of the Slater-Pauling curve.

Half-metallic ferromagnets (HMF) are supposed to exhibit a real gap in the minority density of states and the Fermi energy is pinned inside of the gap. From this point of view, the Slater-Pauling rule is strictly fulfilled with

$$m_{HMF} = n_V - 6 \quad (1)$$

for the magnetic moment per atom, as the number of occupied minority states $n_{d\downarrow}$ has to be integer. The distribution of the minority electrons on different bands, however, has to be found from electronic structure calculations.

For ordered compounds with different kind of atoms it is, indeed, more convenient to work with all atoms of the unit cell. In the case of 4 atoms per unit cell, as in full Heusler (FH) compounds, one has to subtract 24 (6 multiplied by the number of atoms) from the accumulated number of valence electrons in the unit cell N_V (s, d electrons for the transition metals and s, p electrons for the main group element) to find the magnetic moment per unit cell:

$$m_{FH} = N_V - 24. \quad (2)$$

This *valence electron rule*⁴⁵ is strictly fulfilled for HMF only, as was first noted in¹³ for half Heusler (HH) compounds with 3 atoms per unit cell ($m_{HH} = N_V - 18$). In both cases the magnetic moment per unit cell becomes strictly integer (in multiples of Bohr magnetons) for HMF, what may be seen as an advantage of the *valence electron rule* compared to the original Slater-Pauling law (Eq.1) even so it suggests the existence of different laws.

The Slater-Pauling rule relates the magnetic moment with the number of valence electrons per atom^{10,11}, but does not, per se, predict a half-metallic behavior. The gap in the minority states of Heusler compounds has to

be explained by details of the electronic structure (for examples see^{14,15} and references there).

Self consistent field calculations were performed in order to investigate the Slater-Pauling like behavior of Heusler compounds in more detail (for details see Sec.III). The electronic structure of most known Heusler compounds was calculated in order to find their magnetic moments and magnetic type. The calculations were performed for overall 107 reported Heusler compounds from which 59 are based on X and Y being $3d$ metals, 17 with only X and 28 with only Y being a $3d$ metal. The remaining ones contain $4d$ and $4f$ metals on the X and Y sites, respectively. In addition calculations were performed for 50 reported Half-Heusler compounds.

It turned out that nearly all (if not simple metals) Co_2 based compounds should exhibit half-metallic ferromagnetism. It is also found that the calculated magnetic moments of the Co_2 based compounds follow the Slater-Pauling curve as described above (see Fig.1a). Some small deviations are possibly caused by inaccuracies of the numerical integration.

Inspecting the other transition metal based compounds, one finds that compounds with magnetic moments above the expected Slater-Pauling value are $X=Fe$ based. Those with lower values are either $X=Cu$ or $X=Ni$ based, with the Ni based compounds exhibiting higher moments compared to the Cu based compounds at the same number of valence electrons. Moreover, some of the Cu or Ni based compounds are not ferromagnetic independent of the number of valence electrons. Besides Mn_2VAI , only compounds containing both, Fe and Mn , were found to exhibit HMF character with magnetic moments according to the Slater-Pauling rule. No attempts have been made to perform calculations for compounds that turn out to be chemically uncharacterizable.

Inspecting the magnetic data of the known Heusler compounds in more detail (see data and references in^{16,17}), one finds a very interesting aspect. Seemingly, a linear dependence is obtained for Co_2 based Heusler compounds when plotting the Curie temperature (T_C) of the known, $3d$ metal based Heusler compounds as function of their magnetic moment (see Fig.1b). According to this plot, T_C is highest for those half-metallic compounds that exhibit a large magnetic moment, or equivalent for those with a high valence electron concentration as derived from the Slater-Pauling rule. T_C is estimated to be above 1000K for compounds with $6\mu_B$ by an extrapolation from the linear dependence.

Co_2FeSi was revisited as a practical test for the findings above. This compound was previously reported to have a magnetic moment of only $5.18\mu_B$ per unit cell and a Curie temperature of above $980K$ ^{18,19}. One expects, however, $m = 6\mu_B$ and T_C to be above 1000K, from the estimates given above.

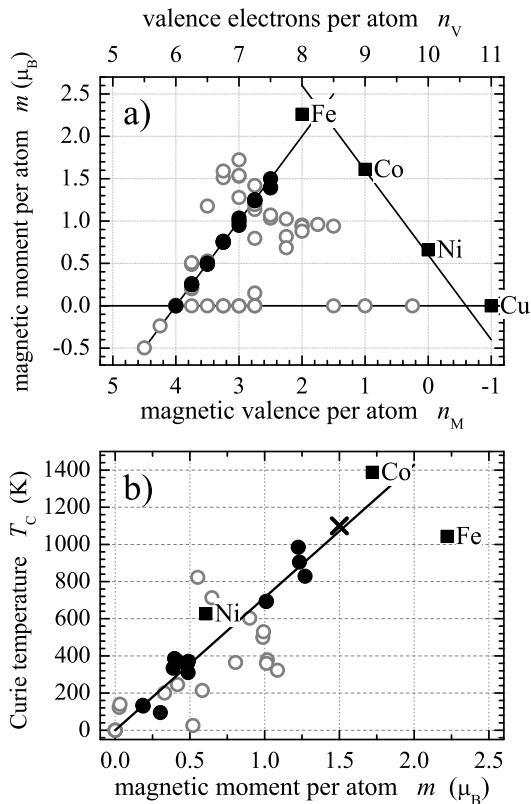


FIG. 1: Magnetic moments (a) and Curie temperature (b) of Heusler compounds.

The heavy 3d transition metals are given for comparison. Full dots assign Co_2 based and open circles assign other Heusler compounds. The lines in a) assign the Slater-Pauling curve. The line in b) is found from a linear fit for Co_2 based compounds. The cross in b) assigns Co_2FeSi as measured in this work.

III. CALCULATIONAL DETAILS

As starting point, self consistent first principle calculations were performed using the linearized muffin tin orbital (LMTO) method²⁰, as this method is very fast. Using the experimental lattice parameter ($a_{exp}=5.64\text{\AA}$, see Sec.V A), the results predicted Co_2FeSi to be a regular ferromagnet with a magnetic moment of $5.08\mu_B$ per formula unit. The latter value is much too small compared to the experimental one of $6\mu_B$ (see Sec.V B).

More detailed calculations were performed to check if the too low value is the result of a particular method or the parameterization of the energy functional. The Korringa-Kohn-Rostocker method as provided by H. Akai²¹ was chosen as this program allows calculations in the muffin tin (MT) and the atomic sphere (ASA) approximations. Additionally, it provides the coherent potential approximation (CPA) to be used for disordered systems. This method was used to estimate the influence

TABLE I: Magnetic moments of Co_2FeSi calculated for spherical potentials.

The calculations were carried out by means of KKR in muffin tin (MT) and atomic sphere (ASA) approximations for $a = 5.64\text{\AA}$. All values are given in μ_B . Total moments are given per unit cell and site resolved values are per atom.

KKR	MT			ASA		
	m_{tot}	m_{Co}	m_{Fe}	m_{tot}	m_{Co}	m_{Fe}
MJW	5.03	1.19	2.69	5.17	1.27	2.68
vBH	4.88	1.15	2.64	5.03	1.22	2.62
VWN	4.99	1.18	2.68	5.15	1.26	2.67
GGA	5.22	1.22	2.85	5.18	1.27	2.69
EV	5.19	1.24	2.77	5.15	1.26	2.68
PYVWN	5.03	1.19	2.72	5.67	1.25	3.23

of disorder on the magnetic structure.

The calculations were started with the most common parameterizations of the exchange-correlation functional as given by Moruzzi, Janak, and Williams²² (MJW), von Barth and Hedin²³ (vBH), and Vosco, Wilk, and Nussair^{24,25} (VWN). The generalized gradient approximation (GGA) was used in the form given by Perdew *et al*²⁶. To include non-local effects, the VWN parametrization with additions by Perdew *et al*^{27,28,29} was used (PYVWN). The so-called exact exchange is supposed to give the correct values for the gap in semi-conductors using local density approximation. Here it was used in the form given by Engel and Vosko³⁰ (EV).

The results of the calculations using different approximations for the potential as well as the parameterization of the exchange-correlation part are summarized in Tab.I. The calculated total magnetic moments range from $\approx 4.9\mu_B$ to $\approx 5.7\mu_B$, thus they are throughout too low compared to the experiment. They include, however, the value of $5.27\mu_B$ found in Ref.¹⁵ by means of the full potential KKR method.

In the next step, the full potential linear augmented plane wave (FLAPW) method as provided by Wien2k³¹ was used to exclude that the observed deviations are due to the spherical approximation for the potential (MT or ASA) as used in the above methods.

First, the exchange-correlation energy functional being parameterized within the generalized gradient approximation was used. The energy convergence criterion was set to 10^{-5} . Simultaneously, the charge convergence was monitored and the calculation was restarted if it was larger than 10^{-3} . For k -space integration, a $20 \times 20 \times 20$ mesh was used resulting in 256 k -points in the irreducible part of the Brillouin zone. In cases of doubt about convergence or quality of the integration, the number of irreducible k -points was doubled.

The calculated magnetic moments for most known Heusler compounds are summarized in Fig.1 and discussed in Sec.II. It turned out, however, that the magnetic moment of Co_2FeSi is still too small compared to

TABLE II: Magnetic moments of Co_2FeSi calculated for full symmetry potentials.

The calculations were carried out by means of FLAPW for $a = 5.64\text{\AA}$. All values are given in μ_B . Total moments are given per unit cell and site resolved values are per atom. m_{int} is the part of the magnetic moment that cannot be attributed to a particular site.

	m_{tot}	m_{Co}	m_{Fe}	m_{Si}	m_{int}
LDA (VWN)	5.59	1.40	2.87	-0.01	-0.07
LDA (EV)	5.72	1.45	2.94	-0.003	-0.11
LDA+ U	6	1.54	3.30	-0.13	-0.25

the experimental value.

Comparing the result for Co_2FeSi , the magnetic moments found by the different calculational schemes are very similar (compare Tabs.I and II), implying that Co and Fe atoms are aligned parallelly independent of the method used. The small, induced moment at the Si atom (not given in Tab.I) is aligned anti-parallelly to that at the transition metal sites. As for KKR, the use of the EV parameterization of the energy functional did not improve the magnetic moment, the result was only $5.72\mu_B$.

Other than the LMTO or KKR methods (spherical potentials), the FLAPW (full symmetry potential) calculations revealed a very small gap in the minority states, but being located below the Fermi energy. Figure 2 shows the band structure and density of states calculated by FLAPW for the experimental lattice parameter.

The electronic structure shown in Fig.2 reveals a very small indirect gap in the minority states at about 2eV below ϵ_F . The fact that the Fermi energy cuts the minority bands above the gap has finally the result that the magnetic moment is too low and not integer, as would be expected for a half-metallic ferromagnet.

A structural refinement was performed to check if the experimental lattice parameter minimizes the total energy. The dependence of the energy with lattice parameter a revealed that the minimum occurs at the experimentally observed lattice parameter a_{exp} . From the lattice parameter dependent calculations it showed up that the experimentally found magnetic moment appears at larger values of a . At the same time the size of the gap increased. Inspecting the band structure, one finds that the Fermi energy is inside of the gap for lattice parameters being enlarged by about 7.5% to 12.5%. Figure 3 shows the dependence of the extremal energies of the lower (valence) band and the upper (conduction) band of the minority states enveloping the gap.

The magnetic moment is integer ($6\mu_B$) in the region where ϵ_F falls into the gap (grey shaded area in Fig.3), that is the region of half-metallic ferromagnetism. The reason for the integer value is clear: the number of filled minority states is integer and thus the magnetic moment, too.

Usually, Heusler compounds are attributed to exhibit localized moments. In that case, electron-electron cor-

TABLE III: Distribution of the valence states in Co_2FeSi .

The number of occupied states was calculated by means of FLAPW using LDA+ U for $a = 5.64\text{\AA}$. The muffin tin radii were set for all sites to $r_{MT} = 1.22\text{\AA}$. This results in a space filling of 67% by the atomic spheres, the remainder is taken as interstitial (int).

	majority	minority
Co	4.887	3.343
Fe	5.063	1.766
Si	1.247	1.373
int	1.915	2.176
sum Co_2FeSi	18	12

relation may play an important rule. The LDA+ U scheme³² was used for calculation of the electronic structure to find out whether the inclusion of correlation resolves the discrepancy between the theoretical and measured magnetic moment. In Wien2k, the effective Coulomb-exchange interaction ($U_{eff} = U - J$, where U and J are the Coulomb and exchange parameter) is used to account for double-counting corrections. It turned out that values of U_{eff} from 2.5eV to 5.0eV for Co and simultaneously 2.4eV to 4.8eV for Fe result in a magnetic moment of $6\mu_B$ and a gap in the minority states.

Figure 4 shows the band structure and density of states calculated using the LDA+ U method. The effective Coulomb-exchange parameter were set to $U_{eff,Co}=4.8\text{eV}$ and $U_{eff,Fe}=4.5\text{eV}$ at the Co and Fe sites, respectively. These values are comparable to those found in Ref.³³ for bcc Fe (4.5eV) and fcc Ni (5eV).

The minority DOS (Fig.4) exhibits a clear gap around ϵ_F , confirming the half-metallic character of the material. The high density below ϵ_F is dominated by d -states being located at Co and Fe sites. Inspecting the majority DOS one finds a small density of states near ϵ_F . This density is mainly derived from states located at Co and Si sites.

The distribution of the charge density on the atoms and states with different orbital momentum is given in Tab.III (Note that two Co atoms count for the sum of the charge in the unit cell.).

From Tab.III it is found that in average three minority states per atom are occupied ($2n_{\downarrow} = 6$) as required by the Slater-Pauling rule for the range of increasing magnetic moments with an increasing number of valence electrons (see Sec.II). It is worthwhile to note that the same is true for the other Heusler compounds shown in Fig.1 exhibiting half-metallic ferromagnetism. However, the electrons are distributed in a different way across the X, Y, and Z sites.

IV. EXPERIMENTAL DETAILS

Co_2FeSi samples were prepared by arc-melting of stoichiometric quantities of the constituents in an argon at-

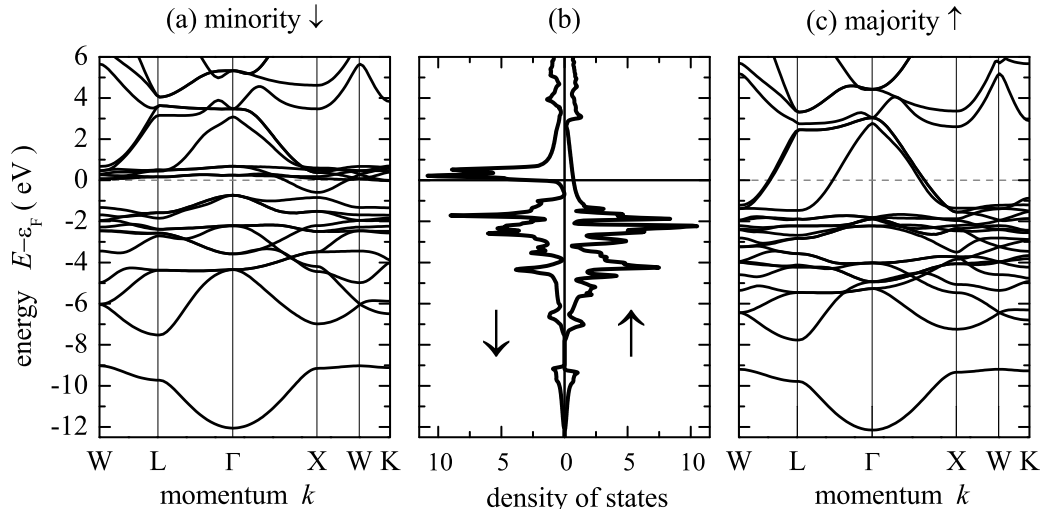


FIG. 2: LDA band structure and DOS of Co_2FeSi . The calculation was performed by Wien2k using the experimental lattice parameter.

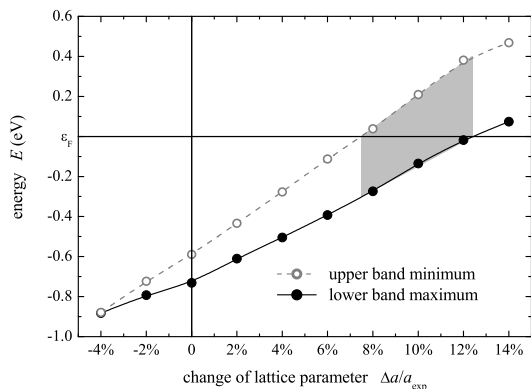


FIG. 3: Minority gap in Co_2FeSi . Shown are the positions of the extremal energies of the upper and lower bands depending on the lattice parameter ($a_{exp} = 5.64\text{\AA}$). Energies are given with respect to the Fermi energy. The grey shaded area marks the domain of HMF character (lines are drawn to guide the eye).

mosphere (10^{-4}mBar). Care was taken to avoid oxygen contamination. This was established by evaporation of Ti inside of the vacuum chamber before melting the compound as well as additional purification of the process gas. Afterwards, the polycrystalline ingots were annealed in an evacuated quartz tube at 1300K for 20 days. This procedure resulted in samples exhibiting the correct Heusler type $L2_1$ structure.

Flat disks were cut from the ingots and polished for spectroscopic investigations at bulk samples. For powder investigations, the remaining part was crushed by

hand using a mortar. It should be noted that pulverizing in a steel ball mill results in strong perturbation of the crystalline structure.

X-ray photo emission (ESCA) was used to verify the composition and to check the cleanliness of the samples. No impurities were detected by means of ESCA after removal of the native oxide from the polished surfaces by Ar^+ ion bombardment.

The geometrical structure was investigated by X-ray diffraction (XRD) using excitation by $\text{Cu-K}\alpha$ or $\text{Mo-K}\alpha$ radiation. Extended X-ray absorption fine structure (EXAFS) measurements were performed at the XAS beamline of LNLS (Campinas, Brazil) for additional structural investigation, in particular to explain the site specific short range order. Powder samples were investigated in transmission mode using two ion chambers, bulk samples were investigated by the total yield technique.

Magneto-structural investigations were carried out by means of Mößbauer spectroscopy in transmission geometry using a constant acceleration spectrometer. A $^{57}\text{Co}(\text{Rh})$ source with a line width of 0.105mm/s was used for excitation.

The magnetic properties were investigated at low temperatures using a super conducting quantum interference device (SQUID, Quantum Design MPMS-XL-5). The high temperature magnetic properties were investigated by means of a vibrating sample magnetometer (Lake Shore Cryotronics, Inc., VSM Model 7300) equipped with a high temperature stage. For site specific magnetometry, X-ray Magnetic Circular Dichroism (XMCD) in photo absorption (XAS) was performed at the *First Dragon* beamline of NSRRC (Hsinchu, Taiwan).

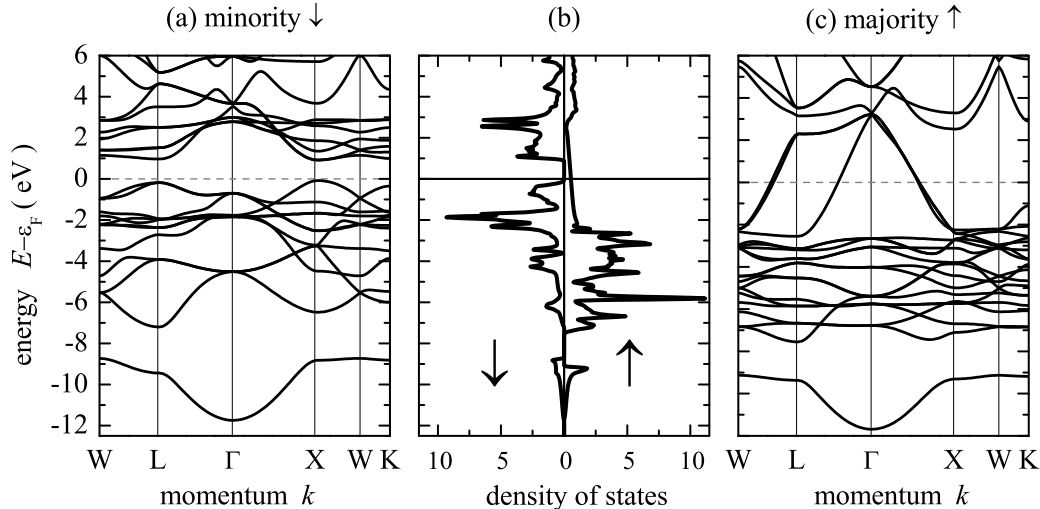


FIG. 4: LDA+ U band structure and DOS of Co_2FeSi . The calculation was performed by Wien2k using the experimental lattice parameter.

V. RESULTS

A. Structural Properties

The correct $L2_1$ structure of the Co_2FeSi compound was verified by XRD. The lattice constant was determined to be 5.64\AA . The lattice parameter is obviously smaller than the one reported before (compare Ref.³⁴) and a lower degree of disorder is observed in the present work.

A disorder between Co and Fe atoms (DO_3 type disorder) can be excluded from the Rietveld refinement of the XRD data, as well as from neutron scattering data (not shown here). A small ($< 10\%$) disorder between Fe and Si atoms ($B2$ type disorder) can not be excluded by either of these methods, particularly due to the low intensities of the (111) and (200) diffraction peaks in XRD.

For further site specific structural information, EXAFS measurements were carried out. A powder sample, as used for XRD, was investigated in transmission mode.

The absorption spectra collected at the Fe and Co K-edges are shown in Fig.5 after removal of a constant background. The ATOMS³⁵ program was used to generate the structural input for the EXAFS data analysis. The scattering parameter for all possible scattering paths were calculated using FEFF6³⁶. The analysis of the EXAFS data was finally performed using the IFEFFIT^{37,38} program package. The best fitting of the Fourier transform modulus considering the $L2_1$ structure are also displayed in Fig.5. It was not possible to fit the experimental data to a structural model including DO_3 type disorder, as expected. $B2$ type disorder can hardly be de-

tected by means of EXAFS as the distances in the first co-ordination shell of Co and Fe are the same as in $L2_1$.

The radial distribution function $\chi(R)$ (FT magnitude) is produced by forward Fourier transform of the EXAFS spectra after background subtraction. It is given as function of the effective distance R . Note that R includes not only the interatomic distances kR_j but also the scattering phase shifts δ_j ($kR_j + \delta_j$). The high intensity of $\chi(R)$ in the first co-ordination shell of Fe points on the cubic environment consisting of eight Co atoms, as expected for a well ordered Heusler compound. The peak of $\chi(R)$ for the first co-ordination shell of Co exhibits a clear splitting being due to the different scattering phases of Fe and Si, although the distance between these atoms and the Co is the same. The Fe induced intensity of $\chi(R)$ is about half of that observed in the Fe K-edge spectra. This confirms the tetragonal environment at the Co sites with respect to Fe sites, as the scattering factors for both types of atoms is nearly the same. Thus, the EXAFS measurements corroborate the XRD results even at the short range order for both Co and Fe.

For additional magneto-structural investigation, Mößbauer spectroscopy was performed. The measurements were carried out at 85K using powder samples. The observed 6-line pattern of the spectrum (see Fig.6) is typical for a magnetically ordered system. The observed ^{57}Fe Mößbauer line width of 0.15mm/s is characteristic for a well-ordered system. The value is comparable to 0.136mm/s observed from $\alpha\text{-Fe}$ at 4.2K.

In detail, the Mößbauer spectrum shown in Fig.6 exhibits a sextet with an isomer shift of 0.23mm/s and a hyperfine magnetic field of $26.3 \times 10^6\text{A/m}$. No paramagnetic line was observed. Further, no quadrupole splitting

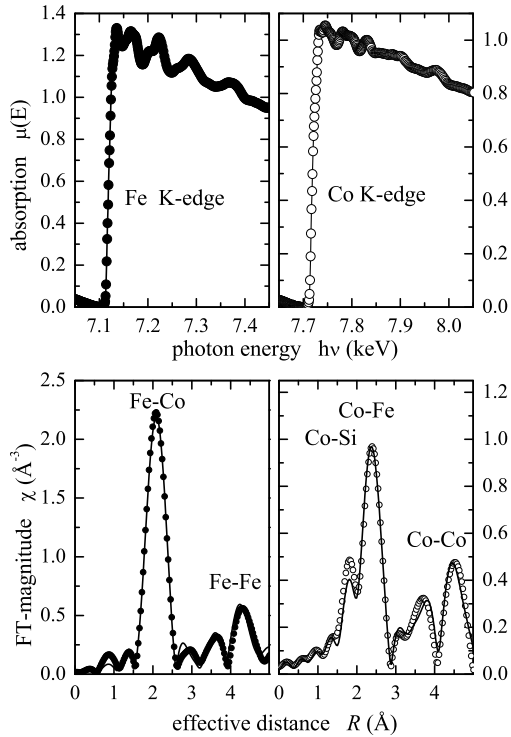


FIG. 5: EXAFS results for Co_2FeSi . The X-ray absorption spectra (with constant background removed) were taken at the K-edges of Co and Fe. The radial distribution functions derived from the spectra (symbols) are compared to the ones calculated (lines) using the best fit data.

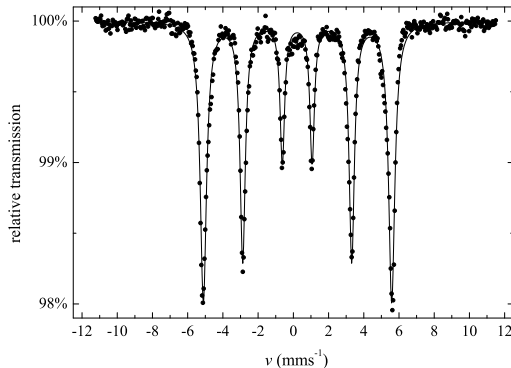


FIG. 6: Mössbauer-spectrum of Co_2FeSi . The spectrum was excited by ^{57}Co and measured from a powder sample in transmission geometry at $T = 85\text{K}$.

was detected in accordance with the cubic symmetry of the local Fe environment. A DO_3 like disorder can be definitely excluded by comparing measured and calculated hyperfine fields in ordered and disordered structures.

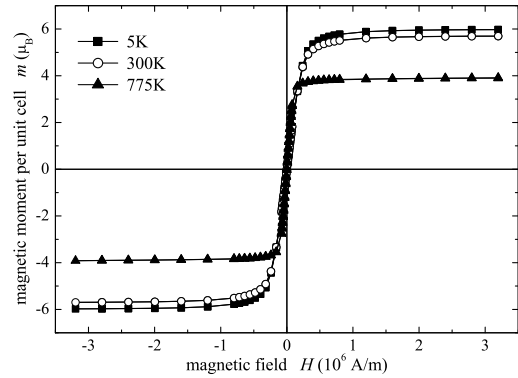


FIG. 7: Magnetic properties of Co_2FeSi . The field dependence of the magnetic moments was measured by SQUID magnetometry at different temperatures.

B. Magnetic Properties

Low temperature magnetometry was performed by means of SQUID to proof the estimated saturation moment. The results are shown in Fig.7. The measured magnetic moment in saturation is $(5.97 \pm 0.05)\mu_B$ at 5K corresponding to $1.49\mu_B$ per atom. An extrapolation to $6\mu_B$ per unit cell at 0K fits perfectly to the one estimated from the Slater-Pauling rule. The measurement of the magnetic moment reveals, as expected for a HMF, an integer within the experimental uncertainty. Regarding the result of the measurement (an integer) and the *valence electron rule*, it all sums up to an evidence for half-metallic ferromagnetism in Co_2FeSi . In more detail, Co_2FeSi turns out to be soft magnetic with a small remanence of $\approx 0.3\%$ of the saturation moment and a small coercive field of $\approx 750\text{A/m}$, under the experimental conditions used here. The magnetic moment for Co_2FeSi was previously reported to be $5.90\mu_B$ ¹⁸ at 10.24K, but with a rather high degree of disorder (11% B_2 and 16% DO_3). The same group reported later³⁴ a smaller magnetic moment ($\approx 5.6\mu_B$ interpolated to 0K) at a lattice parameter of 5.657\AA , but still with a high degree of disorder.

The experimental magnetic moment is supported by the band structure calculations, as was shown above, revealing a HMF character with a magnetic moment of $6\mu_B$, if using appropriate parameters in the self consistent field calculations.

XMCD in photo absorption was measured to investigate the site specific magnetic properties. The XAS and XMCD spectra taken at the $L_{2,3}$ absorption edges of Fe and Co are shown in Fig.8. The feature seen at 3eV below the L_3 absorption edge of Co is related to the L_{21} structure and points on the high structural order of the sample (it vanishes for B_2 like disorder). The magnetic moments per atom derived from a sum rule analysis^{39,40} are $(2.6 \pm 0.1)\mu_B$ for Fe and $(1.2 \pm 0.1)\mu_B$ for Co, at $T = 300\text{K}$ and $\mu_0 H = 0.4\text{T}$. The error arises mainly

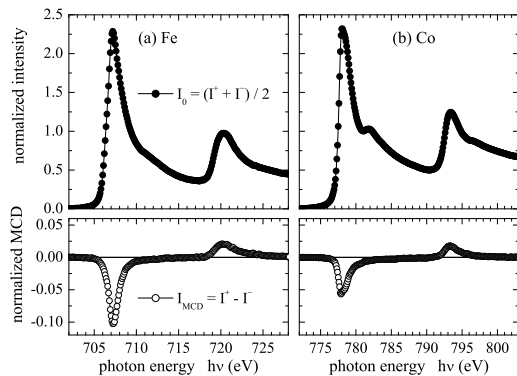


FIG. 8: Site resolved magnetic properties of Co_2FeSi . Shown are the XAS (I_0) and XMCD (I_{MCD}) spectra taken at the $L_{2,3}$ absorption edges of Fe (a) and Co (b) after subtracting a constant background.

from the unknown number of holes in the $3d$ shell and the disregard of the magnetic dipole term in the sum rule analysis. A pronounced enhancement of the orbital magnetic moments (m_l) as in $\text{Co}_2\text{Cr}_{1-x}\text{Fe}_x\text{Al}^{41}$ or a field dependence of m_l ⁴² was not observed for Co_2FeSi .

The orbital moments were calculated using the LDA+ U scheme with spin-orbit interaction (SO) and by LSDA calculations including the Brooks orbital polarization term (OP)⁴³. The LDA+ U calculations with SO revealed $r = m_l/m_s$ values of 0.05 and 0.02 for Co and Fe, respectively. These values are about a factor of two higher than those found from LSDA + SO calculations without U . The total magnetic moment stayed $6\mu_B$ in this calculation as in LDA+ U without SO. The OP calculations revealed slightly higher r values. The orbital to spin magnetic moment ratios determined from the XMCD measurements are about 0.05 for Fe and 0.1 for Co. All values (ratio of Co and Fe moments, as well as values extrapolated to 0K) are in good agreement to the electronic structure calculations, keeping in mind that calculated site resolved values depend always on the RMT-settings for the integration of the charge density around a particular atom.

The high temperature magnetization of Co_2FeSi was measured by means of VSM. The specific magnetization as function of the temperature is shown in Fig.9. The measurements were performed in a constant induction field of $\mu_0 H = 0.1\text{T}$. For this induction field, the specific magnetization at 300K is 37% of the value measured in saturation. The ferromagnetic Curie temperature is found to be $T_C = (1100 \pm 20)\text{K}$. This value fits very well the linear behavior shown in Fig.1 for Co_2 based Heusler compounds.

The Curie temperature is well below the melting point being obtained by means of differential scanning calorimetry to be $T_m = (1520 \pm 5)\text{K}$. The paramagnetic Curie-Weiss temperature was identified to be

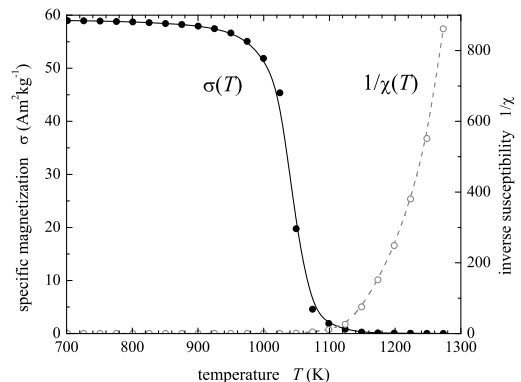


FIG. 9: Measurement of the specific magnetization as a function of temperature for Co_2FeSi . (Lines are drawn to guide the eye).

$\Theta \geq (1150 \pm 50)\text{K}$ from the plot of the inverse susceptibility χ^{-1} as a function of temperature T by interpolating the curve. The non-linearity in the $\chi^{-1}(T)$ dependence close to T_C indicates deviations from molecular field theory. A linear dependence, however, is only expected at temperatures much higher than T_C that are not accessible here.

The highest known Curie temperature is reported for elemental Co to be 1388K⁴⁴. Only few materials exhibit a T_C above 1000K, for example the Fe-Co binary alloys. With a value of $\approx 1100\text{K}$, Co_2FeSi has a higher Curie temperature than Fe and the highest of all HMF and Heusler compounds being measured up to now.

The present work leaves, however, some important questions open. There is still no convincing theory that explains why the dependence of T_C on the magnetic moment should be linear over such a wide range of compounds with different magnetic moments. For some alloys a linear dependence is indeed found, but never over such a wide range of different composition like for the Co_2 based HMF Heusler compounds. An experimental challenge will be to find compounds with magnetic moments of above $6\mu_B$ to prove whether it is possible to find even higher Curie temperatures in this class of materials. Co_3Si , which should exhibit $7\mu_B$, if following the *valence electron rule*, crystallizes in a hexagonal but not in the required Heusler structure, unfortunately.

VI. SUMMARY AND CONCLUSION

In summary, it was shown how simple rules may be used to estimate the properties of magnetic materials, in particular for those Heusler compounds exhibiting half-metallic ferromagnetism.

As practical application of these simple rules, it was found that the Heusler compound Co_2FeSi is a half-metallic ferromagnet exhibiting the highest Curie tem-

perature and magnetic moment. In particular, a magnetic moment of $6\mu_B$ and a Curie temperature of 1100K were found in $L2_1$ ordered samples with a lattice parameter of 5.64\AA .

The experimental findings are well supported by electronic structure calculations. The comparison between experiment and calculations gives clear advise that electron-electron correlation plays an important role in Heusler compounds.

Acknowledgments

We thank Y. Hwu (Academia Sinica, Taipei, Taiwan), M. C. M. Alves (UFRGS, Porto Alegre, Brazil),

H. Seyler, F. Casper (Mainz), and the staff of NSRRC (Hsinchu, Taiwan) and NLNS (Campinas, Brazil) for help with the experiments. We acknowledge assistance of Lake Shore Cryotronics, Inc. with the high temperature magnetic measurements. Further, we thank G. Frisch (Ludwig Alberts - University, Freiburg) for performing Mo- K_α X-Ray diffraction.

This work is financially supported by DFG (research project FG 559), DAAD (03/314973 and 03/23562), PROBRAL (167/04), and LNLS (XAFS1-2372, XAFS1-3304).

-
- * Electronic address: felser@uni-mainz.de
- ¹ J. M. D. Coey, M. Venkatesan, and M. A. Bari, in *Lecture Notes in Physics*, edited by C. Berthier, L. P. Levy, and G. Martinez (Springer-Verlag, Heidelberg, 2002), vol. 595, pp. 377 – 396.
 - ² I. Zutic, J. Fabian, and S. D. Sarma, *Rev. Mod. Phys.* **76**, 323 (2004).
 - ³ R. A. d. Groot, F. M. Müller, P. G. v. Engen, and K. H. J. Buschow, *Phys. Rev. Lett.* **50**, 2024 (1983).
 - ⁴ F. Heusler, *Verh. Dtsch. Phys. Ges.* **12**, 219 (1903).
 - ⁵ K. H. J. Bushow, P. G. v. Engen, and R. Jongebreur, *J. Magn. Magn. Mater.* **38**, 1 (1983).
 - ⁶ S. Ishida, S. Fujii, S. Kashiwagi, and S. Asano, *J. Phys. Soc. Jap.* **64**, 2152 (1995).
 - ⁷ S. Kämmerer, A. Thomas, A. Hütten, and G. Reiss, *Appl. Phys. Lett.* **85**, 79 (2004).
 - ⁸ X. Y. Dong, C. Adelman, J. Q. Xie, C. J. Palmstrom, X. Lou, J. Strand, P. A. Crowell, J.-P. Barnes, and A. K. Petford-Long, *Appl. Phys. Lett.* **86**, 102107 (2005).
 - ⁹ J. Pierre, R. V. Skolozdra, J. Tobola, S. Kaprzyk, C. Hord-equin, M. A. Kouacou, I. Karla, R. Currat, and E. Lelievre-Berna, *J. All. Comp.* **262-263**, 101 (1997).
 - ¹⁰ L. Pauling, *Phys. Rev.* **54**, 899 (1938).
 - ¹¹ J. C. Slater, *Phys. Rev.* **49**, 931 (1936).
 - ¹² A. P. Malozemoff, A. R. Williams, and V. L. Moruzzi, *Phys. Rev. B* **29**, 1620 (1984).
 - ¹³ J. Kübler, *Physica* **127B**, 257 (1984).
 - ¹⁴ J. Kübler, A. R. Williams, and C. B. Sommers, *Phys. Rev. B* **28**, 1745 (1983).
 - ¹⁵ I. Galanakis, P. H. Dederichs, and N. Papanikolaou, *Phys. Rev. B* **66**, 174429 (2002).
 - ¹⁶ P. J. Webster and K. R. A. Ziebeck, in *Alloys and Compounds of d-Elements with Main Group Elements. Part 2*, edited by H. P. J. Wijn (Springer-Verlag, Heidelberg, 1988), vol. 19C of *Landolt-Börnstein - Group III Condensed Matter*, pp. 104 – 185.
 - ¹⁷ K. R. A. Ziebeck and K.-U. Neumann, in *Alloys and Compounds of d-Elements with Main Group Elements. Part 2*, edited by H. P. J. Wijn (Springer-Verlag, Heidelberg, 2001), vol. 32C of *Landolt-Börnstein - Group III Condensed Matter*, pp. 64 – 314.
 - ¹⁸ V. Niculescu, T. J. Burch, K. Rai, and J. I. Budnick, *J. Magn. Magn. Mater.* **5**, 60 (1977).
 - ¹⁹ K. H. J. Buschow, in *Handbook of Magnetic Materials*, edited by E. P. Wolfarth and K. H. J. Buschow (North-Holland, Amsterdam, London, New York, Tokyo, 1988), vol. 4, p. 493.
 - ²⁰ O. Jepsen and O. K. Andersen, *The Stuttgart TB-LMTO-ASA Program version 47* (MPI für Festkörperforschung, Stuttgart, Germany, 2000).
 - ²¹ H. Akai and P. P. Dederichs, *J. Phys. C* **18**, 2455 (1985).
 - ²² V. L. Moruzzi, J. F. Janak, and A. R. Williams, *Calculated Properties of Metals* (Pergamon Press, New York, 1978).
 - ²³ U. v. Barth and L. Hedin, *J. Phys. C: Solid State Phys.* **5**, 1629 (1972).
 - ²⁴ S. H. Vosko, L. Wilk, and M. Nussair, *Can. J. Phys.* **58**, 1200 (1980).
 - ²⁵ S. H. Vosko and L. Wilk, *Phys. Rev. B* **22**, 3812 (1980).
 - ²⁶ J. P. Perdew, J. A. Chevary, S. H. Vosko, K. A. Jackson, M. R. Pederson, D. J. Singh, and C. Fiolhais, *Phys. Rev. B* **46**, 6671 (1992).
 - ²⁷ J. P. Perdew, *Phys. Rev. B* **33**, 8822 (1986).
 - ²⁸ J. P. Perdew and W. Yue, *Phys. Rev. B* **33**, 8800 (1986).
 - ²⁹ P. Mlynarski and D. R. Salahub, *Phys. Rev. B* **43**, 1399 (1991).
 - ³⁰ E. Engel and S. H. Vosko, *Phys. Rev. B* **47**, 13164 (1993).
 - ³¹ P. Blaha, K. Schwarz, G. K. H. Madsen, D. Kvasnicka, and J. Luitz, *WIEN2k, An Augmented Plane Wave + Local Orbitals Program for Calculating Crystal Properties* (Karlheinz Schwarz, Techn. Universitaet Wien, Wien, Austria, 2001).
 - ³² V. I. Anisimov, F. Aryasetiawan, and A. I. Lichtenstein, *J. Phys. Condens. Matter* **9**, 767 (1997).
 - ³³ I. V. Solovyev and M. Imada, *Phys. Rev. B* **71**, 045103 (2005).
 - ³⁴ V. Niculescu, J. I. Budnick, W. A. Hines, K. Rajt, S. Pickart, and S. Skalski, *Phys. Rev. B* **19**, 452 (1979).
 - ³⁵ J. Ravel, *J. Synchrotron Rad.* **8**, 314 (2001).
 - ³⁶ S. I. Zabinsky, J. J. Rehr, A. Ankudinov, R. C. Albers, and M. J. Eller, *Phys. Rev. B* **52**, 2995 (1995).
 - ³⁷ M. Newville, B. Ravel, D. Haskel, J. J. Rehr, E. A. Stern, and Y. Yacoby, *Physica B* **208-209**, 154 (1995).
 - ³⁸ M. Newville, *J. Synchrotron Rad.* **8**, 322 (2001).
 - ³⁹ B. T. Thole, P. Carra, F. Sette, and G. v. d. Laan, *Phys. Rev. Lett.* **68**, 1943 (1992).
 - ⁴⁰ P. Carra, B. T. Thole, M. Altarelli, and X. Wang, *Phys.*

- Rev. Lett. **70**, 694 (1993).
- ⁴¹ H.-J. Elmers, G. H. Fecher, D. Valdaitev, S. A. Nepijko, A. Gloskovskii, G. Jakob, G. Schönhense, S. Wurmehl, T. Block, C. Felser, et al., Phys. Rev. B **67**, 104412 (2003).
- ⁴² H. J. Elmers, S. Wurmehl, G. H. Fecher, G. Jakob, C. Felser, and G. Schönhense, Appl. Phys. A **79**, 557 (2004).
- ⁴³ O. Eriksson, B. Johansson, and M. S. S. Brooks, J. Phys.: Condens. Matter **1**, 4005 (1989).
- ⁴⁴ D. R. Lide, ed., *CRC Handbook of Chemistry and Physics* (CRC Press, Inc, Boca Raton, Florida, 2001), 82nd ed.
- ⁴⁵ This term is used in the following to distinguish the rule derived from the overall number of valence electrons in the unit cell from the more general Slater Pauling.